Title

Polarization of Prostate Cancer-associated Macrophages Is Induced by Milk Fat Globule-EGF Factor 8 (MFG-E8)-mediated Efferocytosis*

Journal

Journal of Biological Chemistry, 289(35)

ISSN

0021-9258

Authors

Soki, Fabiana N
Koh, Amy J
Jones, Jacqueline D
et al.

Publication Date

2014-08-01

DOI

10.1074/jbc.m114.571620

THE JOURNAL OF BIOLOGICAL CHEMISTRY VOL. 289, NO. 35, pp. 24560–24572, August 29, 2014

Polarization of Prostate Cancer-associated Macrophages Is Induced by Milk Fat Globule-EGF Factor 8 (MFG-E8)-mediated Efferocytosis*[S]

Received for publication, April 8, 2014, and in revised form, July 2, 2014 Published, JBC Papers in Press, July 8, 2014, DOI 10.1074/jbc.M114.571620

Fabiana N. Soki[‡], Amy J. Koh[‡], Jacqueline D. Jones[‡], Yeo Won Kim[‡], Jinlu Dai[§¶], Evan T. Keller[§¶], Kenneth J. Pienta[‖1], Kamran Atabai[**], Hernan Roca[‡], and Laurie K. McCauley[‡¶2]

From the [‡]Department of Periodontics and Oral Medicine, University of Michigan School of Dentistry, Ann Arbor, Michigan 48109, the [§]Department of Urology, [¶]Department of Pathology, University of Michigan Medical School, Ann Arbor, Michigan 48109, the [‖]James Buchanan Brady Urological Institute, Johns Hopkins University School of Medicine, Baltimore, Maryland 21287, and the [**]Department of Medicine and Cardiovascular Research Institute, University of California, San Francisco, California 94158

Background: The growing body of data on tumor-associated macrophages largely neglects phagocytosis of apoptotic cells.
Results: MFG-E8, induced during efferocytosis, contributes to macrophage polarization with STAT3/SOCS3 pathway involvement.
Conclusion: Efferocytosis induces macrophage polarization into tumor-associated macrophages mediated by MFG-E8.
Significance: A novel tumor-promoting mechanism for macrophage polarization through efferocytosis and MFG-E8 and its corresponding signaling pathway were identified.

Tumor cells secrete factors that modulate macrophage activation and polarization into M2 type tumor-associated macrophages, which promote tumor growth, progression, and metastasis. The mechanisms that mediate this polarization are not clear. Macrophages are phagocytic cells that participate in the clearance of apoptotic cells, a process known as efferocytosis. Milk fat globule- EGF factor 8 (MFG-E8) is a bridge protein that facilitates efferocytosis and is associated with suppression of proinflammatory responses. This study investigated the hypothesis that MFG-E8-mediated efferocytosis promotes M2 polarization. Tissue and serum exosomes from prostate cancer patients presented higher levels of MFG-E8 compared with controls, a novel finding in human prostate cancer. Coculture of macrophages with apoptotic cancer cells increased efferocytosis, elevated MFG-E8 protein expression levels, and induced macrophage polarization into an alternatively activated M2 phenotype. Administration of antibody against MFG-E8 significantly attenuated the increase in M2 polarization. Inhibition of STAT3 phosphorylation using the inhibitor Stattic decreased efferocytosis and M2 macrophage polarization *in vitro*, with a correlating increase in SOCS3 protein expression. Moreover, MFG-E8 knockdown tumor cells cultured with wild-type or MFG-E8-deficient macrophages resulted in increased SOCS3 expression with decreased STAT3 activation. This suggests that SOCS3 and phospho-STAT3 act in an inversely dependent manner when stimulated by MFG-E8 and efferocytosis. These results uncover a unique role of efferocytosis via MFG-E8 as a mechanism for macrophage polarization into tumor-promoting M2 cells.

The skeleton is a favored organ for metastasis, resulting in significant morbidity for cancer patients (1, 2). Tumor-associated macrophages (TAMs)[3] have been investigated in the context of cancer (3, 4), but their role in bone metastasis remains elusive (3, 5, 6). Macrophages are activated differentially according to the stimuli provided. M1 antitumorigenic macrophages are defined as classically activated, and M2 protumorigenic macrophages (also known as TAMs) are defined as alternatively activated (7, 8). TAMs are prominently involved with cancer initiation, progression, and metastasis, facilitating angiogenesis, matrix breakdown, and tumor cell motility (9–11). Although the role of TAMs in skeletal metastasis is emerging, the mechanisms remain to be defined.

In addition to their high rate of cell proliferation, tumors have high apoptosis rates, an often forgotten but important process in tumor dynamics (12). The large number of apoptotic cells is underappreciated because of rapid cell clearance performed by macrophages and other phagocytic cells, a process known as efferocytosis. Indeed, not much is known regarding the interactions of apoptotic tumor cells with macrophages and, subsequently, how this affects the remaining viable tumor cells in skeletal metastasis. Efferocytosis elicits changes in immune responses and can result in immunosuppression of antitumor defenses (13, 14); production of anti-inflammatory mediators, including TGF-β and IL-10; and inhibition of proinflammatory TNF (14, 15).

* This work was supported by Fund for Cancer Research grants and by National Cancer Institute Grants P01-CA093900 (to L. K. M., K. J.P., and E. T. K.) and F32 CA 168269 (to F. S.).
[S] This article contains supplemental Movies 1 and 2.
[1] Supported as an American Cancer Society Clinical Research Professor by Grants U01CA143055 and U54CA143803.
[2] To whom correspondence should be addressed: University of Michigan School of Dentistry, 1011 N. University Ave., Ann Arbor, MI 48109. Tel.: 734-763-3311; Fax: 734-763-5503; E-mail: mccauley@umich.edu.

[3] The abbreviations used are: TAM, tumor-associated macrophage; MFG, milk fat globule; PS, phosphatidylserine; HAP, high apoptotic; BAP, basal apoptotic; TMA, tissue microarray; BPA, benign prostatic hyperplasia; CFSE, carboxyfluorescein succinimidyl ester.

Milk fat globule-EGF factor 8 (MFG-E8) is a protein secreted by numerous cells including macrophages and is known as a phagocytosis "eat me" signal (16, 17). MFG-E8 functions as a tether between macrophage and apoptotic cells via a bimotif function, binding to both phosphatidylserine (PS) externalized on apoptotic cells and the $\alpha_v\beta_3/\alpha_v\beta_5$ integrin expressed on macrophages (16). MFG-E8 mutant mice are deficient in efferocytosis, resulting in increased apoptotic cell accumulation, which has been implicated in autoimmunity- and inflammatory-related diseases (18–20).

Interestingly, phagocytes activated by their interaction with apoptotic cells via MFG-E8 share similar anti-inflammatory and tumor-promoting properties, as seen in M2 TAMs (7, 12, 21). Pretreatment of LPS-stimulated macrophages with rMFG-E8 results in activation of suppressor of cytokine signaling 3 (SOCS3) via the STAT3 pathway (22). SOCS3 proteins are known to inhibit the JAK/STAT signaling pathway, creating a negative feedback loop to prevent excessive activation of the pathway (23). This modulatory role has also been suggested as a mechanism for macrophage polarization. Despite these suggestive links, efferocytosis via MFG-E8 and its role in tumor efferocytosis and M2 polarization has not been investigated in the context of prostate cancer or skeletal metastasis.

Given that prostate cancer has a high propensity to metastasize to the bone, which is rich in macrophages and anti-inflammatory factors that contribute to tumor growth, we hypothesized that MFG-E8-mediated efferocytosis modulates the bone marrow-derived macrophage SOCS3/STAT3 pathway, inducing an M2 switch and promoting tumor growth. In this study, the impact of efferocytosis mediated by MFG-E8 on macrophage polarization into M2 TAMs was investigated, and the underlying mechanisms that could be developed as potential therapeutic targets were delineated.

EXPERIMENTAL PROCEDURES

Primary Cells and Cell Lines—All animals were maintained in accordance with institutional animal care and use guidelines, and experimental protocols were approved by the Institutional Animal Care and Use Committee of the University of Michigan. MFG-E8 mutant mice were provided by Kamran Atabai from the University of California, San Francisco. Briefly, MFG-E8 mutant mice have an insertion of the pGT1-pfs gene trap vector in intron 7 of Mfge8, trapping the secretory protein, resulting in fusion protein degradation in the endoplasmic reticulum (24).

Primary bone marrow cells were collected from male C57BL/6J (The Jackson Laboratory, Bar Harbor, ME) and MFG-E8 mutant mice at 4–6 weeks of age for *in vitro* experiments. Mouse bone marrow macrophages were differentiated *in vitro* from bone marrow cells cultured in α-minimal essential medium (MEM) with 30 ng/ml murine M-CSF (eBioscience) for 6 days. At day 7, macrophages or RAW 264.7 cells were plated into 12-well plates. Cells were treated with recombinant murine MFG-E8 (R&D Systems) at the indicated concentrations. Anti-MFG-E8 (D161--3, MBL International) and IgG control (Dako) were used at 20 μg/ml to treat macrophages *in vitro* as described previously (25).

Three prostate cancer cell lines were used in this study. Two human bone metastatic prostate cancer cell lines, C42B and PC-3, were obtained from the ATCC. RM-1, a murine cell line, was originally obtained from Dr. Timothy C. Thompson (Baylor College of Medicine, Houston, TX). C42B cells, originally derived from LNCaP tumors maintained in castrated and intact athymic male mice, are androgen-independent, metastasize to the bone, and form mixed osteoblastic/osteolytic lesions (26). PC-3 cells, derived from human vertebral prostate cancer metastasis, are androgen-independent, highly metastatic, and produce osteolytic lesions. Human PC-3 cells were stably transfected to express dsGREEN immunofluorescence.

Apoptosis of prostate cancer cells (RM-1, PC-3, and C42B) was induced by overnight serum starvation followed by 24-h treatment with cobalt chloride (RM-1, 150 μM; PC-3 and C42b, 200 μM) (Sigma-Aldrich). Cells were washed at least three times with PBS after apoptosis induction and enumerated. A 60–70% range of trypan blue-positive cells was designated high apoptotic (HAP). UV exposure of tumor cells for 20 min in PBS was also utilized to induce apoptosis, avoiding chemical-derived effects. Untreated tumor cells contained 5–10% trypan blue-positive cells and were designated as basal apoptotic (BAP) cells.

Stable shRNA Constructs—Mouse GIPZ lentiviral shRNAmir was transfected into RM-1 prostate cancer cells to produce MFG-E8-shRNA stable constructs. Cells were designated as RM-1 m_08 (clone ID V2LMM_277508), RM-1 m_30 (clone ID V2LMM_39830), RM-1 m_41 (clone ID V3LMM_432041), RM-1 m_43 (clone ID V3LMM_432043), RM-1 m_45 (clone ID V3LMM_432045), and RM-1 GIPZ scramble control (LentipGipZ-scramble-VSVG, University of Michigan Vector Core).

Efferocytosis Assay—RAW 264.7 cells or primary bone marrow macrophages were plated at 50,000 cells/cm^2 and incubated at different time points with low or high apoptotic prostate cancer cells (RM-1, PC-3, and C42b) at a 1:3 ratio of macrophage to tumor cells or carboxylated fluorescent beads (Bangs Laboratories, Inc.) at a 1:2 ratio. Cells were washed with PBS, and attached cells were collected for further analyses.

Confocal Microscopy—Bone marrow macrophages, RAW 264.7 cells and prostate cancer cells were stained with 0.2 μl/ml orange or green CellTracker™ or CellTrace™ carboxyfluorescein succinimidyl ester (Invitrogen) for 20 min in serum-free medium, followed by incubation in complete medium for 60 min. Macrophages were plated in 1.5-mm coverglass chambers for confocal microscopy. High apoptotic cancer cells or carboxylated fluorescent beads were added at a 1:1 or 1:2 ratio to the attached macrophages for up to 24 h and fixed with ice-cold methanol for 20 min. Cells were then washed with PBS and covered with Vectashield® mounting medium containing DAPI (Vector Laboratories, Inc.). Confocal microscopy images were analyzed using the Leica inverted SP5X confocal microscope system with two-photon film and Leica software (Leica Microsystems, Germany).

Flow Cytometry—Flow cytometry was performed as described previously (27). Briefly, cells were collected in FACS buffer (PBS, 2% FBS, and 2 mM EDTA), and 1 million cells were stained for 30 min with the following macrophage-specific antibodies: F4/80 Alexa Fluor 647 (Abcam, CI:A3-1) and CD206 PE (AbD Serotec, MR5D3). Cells were fixed and permeabilized with Leucoperm™ (AbD Serotec) and incubated with anti-

Ym1 rabbit antibody (StemCell Technologies, catalog no. 01404). Cells were then incubated with secondary antibody, Alexa Fluor 700 goat anti-rabbit IgG (Molecular Probes) 700. For confirmation of apoptosis, prostate cancer cells were stained with the FITC annexin V apoptosis detection kit (BD Biosciences). After antibody incubation, cells were washed twice with FACS buffer, fixed with 1% formalin, and evaluated for FACS analyses (BD FACSAria^{TM} III).

Western Blot Analyses and Quantification—For protein collection, cells were washed twice with cold PBS and lysed with CelLytic^{TM} MT (Sigma). SDS-PAGE was performed in 4–20% gradient Novex Tris-glycine gels (Invitrogen) loaded with 50 μg of protein/well. After electrophoresis, proteins were transferred to membranes (Duralon UV membrane, Stratagene) and blocked in 5% milk for 20 min. The membranes were then incubated with the primary antibody in 5% milk overnight on a shaker at 4 °C. Antibodies against β-actin (C4) 1:50,000 (Santa Cruz Biotechnology, Inc.), SOCS3 (1:500 dilution, Cell Signaling Technology), phospho-STAT3 (3E2) and STAT3 (124H6, 1:1000 dilution, Cell Signaling Technology), and MFG-E8 (1:500, R&D Systems) were used. After washing, membranes were incubated with secondary antibodies, washed, and then chemiluminescence (via SuperSignal West Pico chemiluminescent substrate, Thermo Scientific) was imaged on x-ray film. Protein quantification was performed using the Scion Image software and calculated relative to control protein expression (β-actin).

RNA Extraction and Quantitative RT-PCR—RNA isolation was performed as described previously (28) using an RNeasy mini kit (Qiagen, Valencia, CA). cDNA was synthesized using 0.5 μg of total RNA in 50 μl of reaction volume using the TaqMan reverse transcription kit (Applied Biosystems). Quantitative real-time PCR was performed using the ABI PRISM 7700 using a ready-to-use mix of primers and FAM-labeled probe assay systems (Applied Biosystems) for *Il10* (Mm00439614_m1), transforming growth factor β1 (*Tgf-β1*, Mm03024053_m1), *Ym1* (*Chi3l3*, Mm00657889_mH), and arginase 1 (*Arg1*, Mm00475988_m1). GAPDH (*Gapdh*, Mm99999915_g1) was used as an internal reference, and the ΔΔCT method was used to calculate the data as described previously (29).

Immunohistochemistry—A prostate cancer tissue microarray (TMA) was obtained through the rapid autopsy program at the University of Michigan Prostate Cancer Specialized Program of Research Excellence Tissue Core. The institutional review board at the University of Michigan approved the use of all tissues. A total of 30 benign ($n = 12$) and malignant ($n = 18$) paraffin-embedded tissue specimens were analyzed with a Gleason score of 7 to 8. Areas of malignant and benign prostatic hyperplasia (BPH) were taken from the same patients (matched paired tissues). Immunohistochemical detection of human MFG-E8 and CD68 (KP1) was carried out in deparaffinized and rehydrated sections using the HRP-AEC cell and tissue staining kit (R&D Systems) according to the protocol of the manufacturer. Tissue was permeabilized with 0.2% Triton X-100 and incubated overnight at 4 °C with anti-mouse CD68 (1:200) and anti-human MFG-E8 (1:50) (Abcam). Samples were counterstained with hematoxylin and mounted with paramount aqueous mounting medium (Dako). Negative controls were used to detect nonspecific staining. MFG-E8 staining was quantified using NIS Elements software (Nikon). Briefly, the region of interest tool was used to set the target area that was positively stained for MFG-E8 over the total area (percent) of the tissue. The mean area positive for MFG-E8 was then calculated for each tissue within three different areas of tissue. The proximity of CD68+ cells to MFG-E8 expression was determined by analyzing three tissue sections at ×100 magnification per specimen per TMA. Cells overlapping or in close proximity that were positive for both CD68 (macrophage) and MFG-E8 expression were quantified using ImageJ software.

Serum Exosomes—Serum samples were obtained from subjects through a protocol approved by the University of Michigan institutional review board. Blood serum was isolated from patients with primary ($n = 6$), metastatic prostate cancer ($n = 7$), or control tumor-free ($n = 3$). Human serum was centrifuged at 500 × *g* for 10 min, after which the resultant supernatant was centrifuged at 20,000 × *g* for 20 min. Exosomes were then harvested by centrifugation at 100,000 × *g* for 70 min (Sorvall S100-AT5 rotor). The exosome pellet was resuspended in PBS, filtered through 0.2-μm nylon filters (GE) and collected by ultracentrifugation at 100,000 × *g* for 70 min. Exosomes were lysed with radioimmune precipitation assay lysis buffer (Millipore, Billerica, MA) containing a complete protease inhibitor tablet (Sigma). Lysates were cleared by centrifugation at 14,000 × *g* for 20 min. 50 μg of protein was loaded in 4–20% gradient Novex Tris-glycine gels, and Western blot analysis was performed as described above. MFG-E8 protein expression was quantified using the Scion Image software and calculated relative to control GAPDH.

Mouse Inflammation Antibody Array—Bone marrow macrophages were plated into 6-well dishes (3×10^6 cells/well). After 24 h, cells were washed with PBS, and 1% FBS α-minimal essential medium was added to the wells with or without high apoptotic RM-1 cells at a 1:1 ratio. The supernatant was collected after 24 h, and proteins were analyzed using the mouse inflammation antibody array C1 (catalog no. AAM-INF-1–8, RayBiotech, Inc.) following the instructions of the manufacturer.

Statistical Analyses—Statistical analysis was performed by unpaired Student's *t* test to compare two groups with a significance of $p < 0.05$. Data are presented as mean ± S.E.

RESULTS

MFG-E8 Is Highly Expressed in Prostate Cancer—MFG-E8 has been correlated with tumor growth and progression of different types of cancers, such as melanoma and breast cancer, but its expression in prostate cancer is still unclear. To elucidate the pattern of MFG-E8 in prostate cancer, immunohistochemistry was performed on serial sections of prostate cancer patient-derived TMAs containing a total of 30 benign ($n = 12$) and malignant ($n = 18$) tissue specimens combined (Fig. 1, *A* and *B*). MFG-E8 expression was significantly higher in malignant (31.93% ± 1.27) compared with benign (4.89% ± 0.68) tissues (Fig. 1*A*). MFG-E8 appeared to be localized on the plasma membrane and in the cytoplasm. However, invasive specimens revealed intense MFG-E8 at the leading edge of tumors and in the apical and basal areas

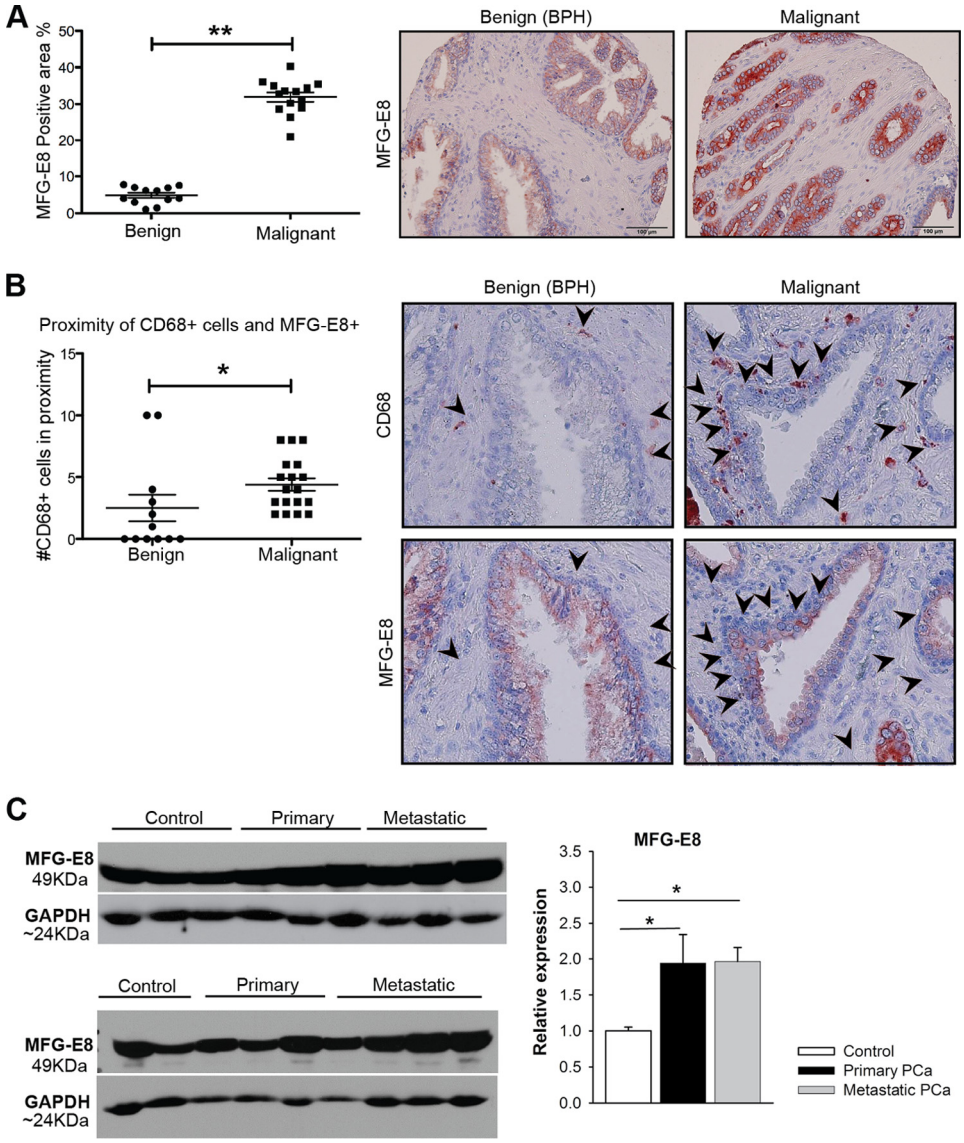

FIGURE 1. **MFG-E8 expression is increased in prostate cancer patients.** *A* and *B*, immunohistochemistry was performed on serial sections of prostate cancer TMAs containing 30 benign ($n = 12$) and malignant ($n = 18$) matched tissue specimens combined. *A*, MFG-E8 expression in benign and malignant prostate cancer TMAs was analyzed by calculation of percent positive MFG-E8 expression in the region of interest. Data are mean ± S.E. **, $p < 0.0001$. *B*, proximity of CD68-positive macrophages and MFG-E8 was determined by analyzing three tissue sections at ×200 magnification per specimen per TMA. Overlapping or cells in close proximity positive for CD68 and MFG-E8 were counted, as indicated by *arrowheads*. The number (#) of CD68+ cells in proximity to MFG-E8 was counted as indicated in the graph. The mean of all three images was calculated, and the overall mean was obtained for each tissue type. Data are mean ± S.E. *, $p < 0.05$. *C*, serum exosome proteins were isolated from patients with primary ($n = 6$) and metastatic ($n = 7$) prostate cancer (*PCa*) or control tumor-free individuals ($n = 3$). The first two controls from the *top blot* were also included in the *bottom blot* for standardization and relative calculation. MFG-E8 protein expression was quantified using Scion Image software and calculated relative to control GAPDH. Data are mean ± S.E. *, $p < 0.05$.

of luminal epithelial cells. The proximity of CD68+ cells to MFG-E8 expression was determined to be two times higher in malignant specimens (Fig. 1*B*). The increased proximity of CD68+ cells in areas of high MFG-E8 expression indicates a potential interaction between MFG-E8 and macrophages in prostate cancer.

Protein expression levels were investigated in blood exosomes isolated from patients with prostate cancer or non-cancer controls (Fig. 1*C*). Blood was collected from patients with localized primary prostate cancer or castration-resistant cancer patients with metastases (30). Western blot analyses revealed that MFG-E8 levels were increased significantly in patients that presented with primary and metastatic prostate cancer. Taken together, these data suggest that MFG-E8 is a potential marker for prostate cancer progression.

MFG-E8 Is Increased in Macrophages during Efferocytosis of Apoptotic Cells—MFG-E8 is a protein that mediates the interaction of macrophages and apoptotic cells, thereby facilitating efferocytosis. To evaluate efferocytosis of apoptotic tumor cells by macrophages, bone marrow macrophages were cultured with tumor cells, and efferocytosis was investigated. RM-1 cells stained with Cell Tracker dye (CFSE+ green) and treated with $CoCl_2$ to induce apoptosis were designated as HAP cells (>60% apoptosis). Untreated cells (<10% apoptosis) were designated as BAP cells and used as controls. Fig. 2*A* shows representative confocal microscopic images of macrophages (*red*) coincu-

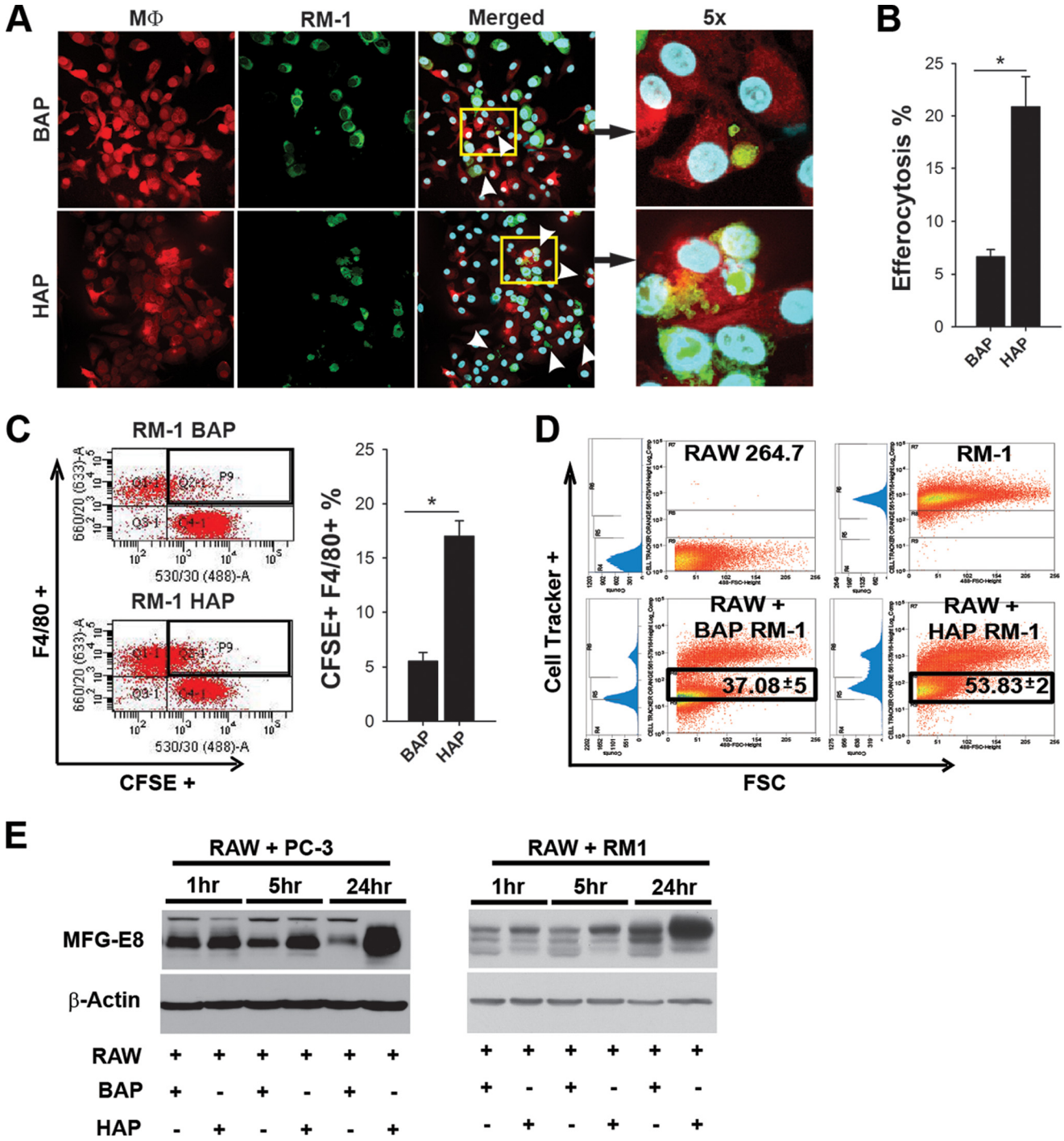

FIGURE 2. **Efferocytosis of apoptotic tumor cells and MFG-E8 expression.** *A*, representative confocal images (×63, 1.4 oil objective) of stained macrophages (*Mϕ*, *red*) cocultured for 5 h with CFSE-stained HAP (>60% apoptosis) and BAP (<10% apoptosis) RM-1 prostate cancer cells (*green*) at a 1:1 ratio. DAPI nuclear staining is shown in *blue*. *White arrowheads* show colocalization suggesting efferocytosis. *B*, quantification of efferocytosis in four fields of confocal microscopic images. Macrophages were cocultured with HAP or BAP RM-1 cells. Data are mean ± S.E. ($n = 4$/group). *, $p < 0.05$. *C*, flow cytometric analyses of bone marrow macrophages cultured with CFSE-stained RM-1 cells with basal or high apoptosis for 5 h. A representative plot shows cells double-positive for CFSE and the macrophage marker F4/80 indicating efferocytosis. The graph shows collective data (mean ± S.E., $n = 5$/group). *, $p < 0.05$. *D*, flow cytometric analyses of efferocytosis. Unstained RAW 264.7 cells cocultured for 5 h with Cell Tracker-stained HAP (>60% apoptosis) and BAP (<10% apoptosis) RM-1 cells. Efferocytosis was measured on the basis of unstained macrophages engulfing the RM1 Cell Tracker+ cells described as percent total cells ± S.E. ($n = 5$/group, $p < 0.05$). *FSC*, forward scatter. *E*, MFG-E8 is increased in macrophages cultured with high apoptotic RM-1 and PC-3 cells. Shown is a Western blot analysis for MFG-E8 protein expression when RAW 264.7 cells were cultured with BAP or HAP for 1, 5, and 24 h of incubation.

bated with RM-1 cells (CFSE+ green). Efferocytosis was quantified relative to the number of nuclei (DAPI) and was increased significantly when macrophages were cultured with HAP cells *versus* control BAP tumor cells (Fig. 2*B*). Confocal microscopic images of bone marrow macrophages confirmed efferocytosis as shown in supplemental Movies 1 and 2 (Z stack videos). Increased efferocytosis of HAP cells compared with control (BAP) cells was also observed by flow cytometry quantification.

F4/80+ bone marrow macrophages that engulfed CFSE+ tumor cells were analyzed as shown in Fig. 2*C*.

Efferocytosis was also analyzed in unstained RAW 264.7 (RAW) macrophages that were cocultured with RM-1 HAP or BAP for 5 h. Efferocytosis of RM-1 cells by macrophages was measured by flow cytometric analysis on the basis of RAW cell engulfment of Cell Tracker-stained RM-1 cells (Fig. 2*D*). Efferocytosis was increased when macrophages were cultured with RM-1 HAP compared with control BAP tumor cells.

MFG-E8 functions as a facilitator of efferocytosis, binding to PS expressed on apoptotic cells and to the $\alpha_v\beta_3/\alpha_v\beta_5$ integrin expressed on macrophages (16). To determine whether increased efferocytosis would affect MFG-E8 expression in macrophages, RAW cells were cultured with low or high apoptotic tumor cells at different time points, and MFG-E8 protein expression was determined (Fig. 2*E*). Western blot analyses showed that MFG-E8 protein expression increased over time and was augmented when cells were cultured with HAP tumor cells. Taken together, these data suggest that coincubation of macrophages with apoptotic tumor cells elicits efferocytosis and increased MFG-E8 levels.

MFG-E8 Expression in Macrophages and Tumor-derived MFG-E8—Although MFG-E8 is expressed in many tissues and cells, its expression in prostate cancer cell lines has remained unknown (31). To determine whether MFG-E8 is expressed in prostate cancer cells, protein was collected and analyzed from RAW 264.7 macrophages and three different prostate cancer cell lines: a prostate cancer murine-derived cell line, RM-1, and two bone metastatic human-derived cell lines, PC-3 and C42B (Fig. 3*A*). MFG-E8 expression was increased in HAP *versus* BAP RM-1 cells but did not change significantly for HAP PC-3 and C42b cells *versus* BAP cells. Overall, all cell lines tested highly expressed MFG-E8.

Because high apoptotic RM-1 cells express high levels of MFG-E8, the contribution of macrophage-derived MFG-E8 during efferocytosis was investigated further. Bone marrow macrophages from C57BL/6J WT or MFG-E8 mutant mice lacking functional secreted MFG-E8 (KO) were expanded, and MFG-E8 protein levels were confirmed (Fig. 3*B*). To determine whether efferocytosis increased MFG-E8 expression in macrophages without the interference of tumor-derived MFG-E8, stable-shRNA RM-1 constructs were generated using five different clones and a pGIPZ scramble clone as control (*RM-1 GIPZ*) (Fig. 3*C*). The clones with higher efficiency of MFG-E8 knockdown, RM-1 m_08 and RM-1 m_30, were selected for further analyses. Bone marrow macrophages from WT and mutant (KO) mice were cocultured with BAP or HAP cells from shRNA or scramble controls for 5 h (Fig. 3*C*). Interestingly, MFG-E8 protein levels were increased when WT macrophages were cultured with HAP cells from control (GIPZ) and shRNA clones (m_08 and m_30) but not detected when the KO cells were cultured with high apoptotic cells (Fig. 3, *D* and *E*). This suggests that, even though RM-1 cancer cells express MFG-E8, efferocytosis elicits the production of MFG-E8 in macrophages.

Efferocytosis of Apoptotic Prostate Cancer Cells Induces M2 Polarization in Macrophages—Because efferocytosis stimulates MFG-E8 in macrophages and given the role of MFG-E8 as a potential immune modulator in macrophages, it was hypothesized that MFG-E8-mediated efferocytosis could be a possible mechanism for macrophage polarization into the M2 type. To better elucidate whether efferocytosis of tumor cells plays a role

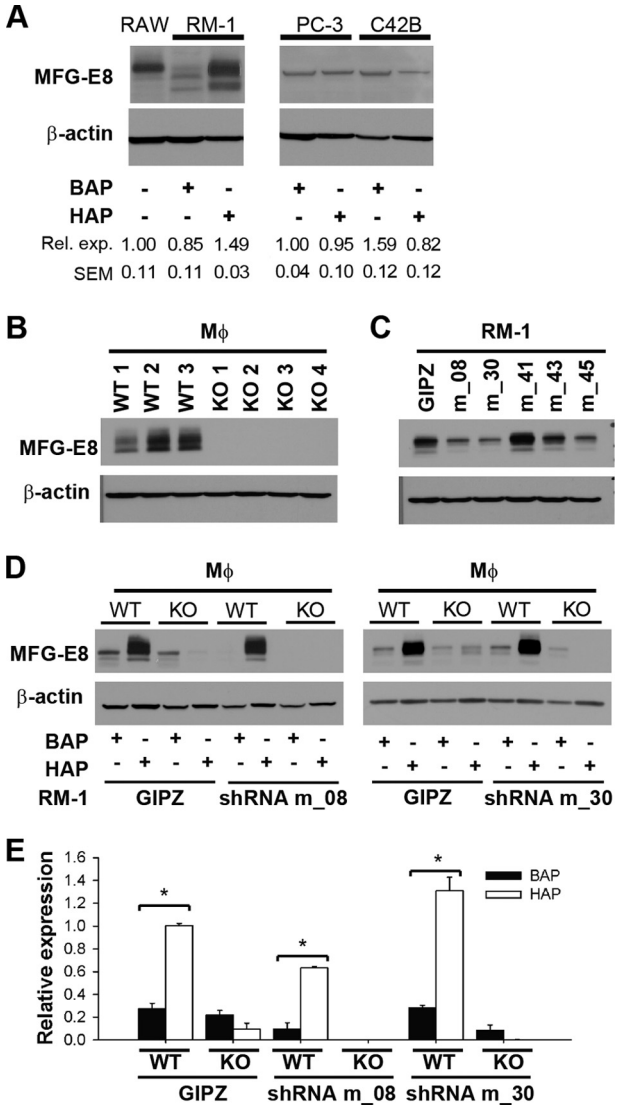

FIGURE 3. **Macrophage-derived MFG-E8 expression is increased during efferocytosis regardless of tumor-derived MFG-E8 expression.** *A*, MFG-E8 expression in prostate cancer and macrophage cell cultures. Shown is expression of MFG-E8 in cells alone. RAW 264.7 macrophages (*RAW*), RM-1, PC-3, and C42B prostate cancer cells express MFG-E8. Prostate cancer cells were treated with $CoCl_2$ for 24 h (>60% apoptosis) and designated as HAP. BAP cells were left untreated (<10% apoptosis). Proteins were analyzed by Western blotting. Expression is reported relative to corresponding β-actin levels. Shown is a representative blot of two independent experiments where values correspond to fold change relative to RAW control (for RM1) or to PC-3 (for PC-3 and C42B). Data are mean ± S.E. (*SEM*) ($n = 2$/group). *Rel. exp.*, relative expression. *B*, MFG-E8 protein expression from bone marrow macrophages collected from C57Bl/6 WT or MFG-E8 KO. *C*, MFG-E8 stable knockdown in cells was generated using five different clones as described under "Experimental Procedures." Protein expression indicated the greatest knockdown for MFG-E8 in clones m_08 and m_30. *D*, WT or KO macrophages were cultured with BAP or HAP RM-1 cells containing GIPZ (negative control) or clone shRNA (*m_08* and *m_30*) for 5 h at a 1:1 ratio. A representative image for Western blot analyses is shown, and MFG-E8 expression was determined. Experiments were repeated twice with similar results. *E*, quantification for MFG-E8 expression was determined by relative expression of MFG-E8 to the control β-actin. Data are mean ± S.E. of two independent experiments and normalized to HAP WT GIPZ control ($n = 2$/group). *, $p < 0.05$.

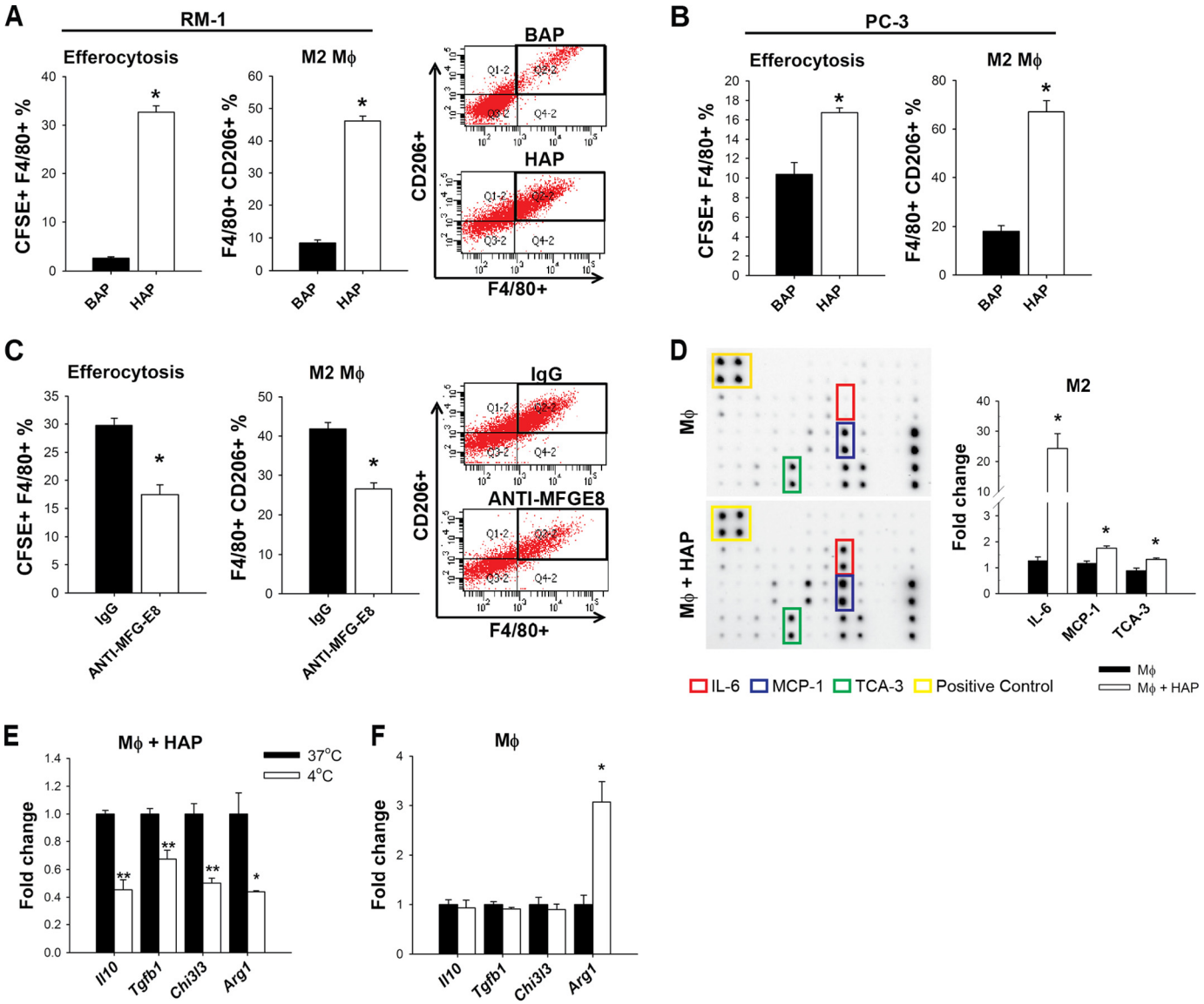

FIGURE 4. **Efferocytosis via MFG-E8 induces M2 polarization.** *A* and *B*, FACS analyses of efferocytosis in bone marrow macrophages (*Mϕ*) cultured with BAP or HAP RM-1 (*A*) or PC-3 (*B*) cells. Efferocytosis was demonstrated as double-positive cells (*CFSE+F4/80+*) indicating macrophages (*F4/80+*) that engulfed tumor cells (*CFSE+*). Representative FACS and M2 polarization is shown as F4/80+CD206+ cells. Data are mean ± S.E. ($n = 4$/group from three independent experiments). *, $p < 0.05$. *C*, macrophages were treated with IgG or anti-MFG-E8 (20 μg/ml) and then cocultured with HAP RM-1 cells. FACS analyses of efferocytosis, reported as double-positive cells (*CFSE+F4/80+*) and M2 polarization (*F4/80+CD206+*) and representative FACS are shown. Data are mean ± S.E. ($n = 4$/group). *, $p < 0.05$ from three independent experiments. *D*, bone marrow macrophages were cultured for 24 h with HAP RM-1 cells or not cultured. The supernatant was collected, and proteins were analyzed using a mouse inflammation antibody array. The fold increase in densitometry was calculated relative to the positive controls (*yellow*) and according to the protocol of the manufacturer. Shown are IL-6 (*red*), chemokine (C-C motif) ligand 2 (CCL2 or MCP-1, *blue*), and chemokine (C-C motif) ligand 1 (CCL1 or TCA-3, *green*). Data are mean ± S.E. ($n = 3$/group). *, $p < 0.05$ from three independent experiments. *E*, bone marrow macrophages were cultured for 5 h with HAP RM-1 cells at 37 °C or at 4 °C to block efferocytosis. Gene expression levels were analyzed by quantitative PCR relative to *Gapdh*, and fold change was calculated. Shown are interleukin 10 (*Il10*), transforming growth factor β 1 (*Tgfb1*), Ym-1 (also known as chitinase 3-like protein 3, *Chi3l3*), and arginase1 (*Arg1*). Data are mean ± S.E. ($n = 6$/group from two independent experiments). *, $p < 0.05$; **, $p < 0.001$. *F*, bone marrow macrophages incubated at 4 °C did not alter gene expression. Gene expression relative to *Gapdh* and fold change was calculated for interleukin 10 (*Il10*), transforming growth factor β 1 (*Tgfb1*), Ym-1(*Chi3l3*), and arginase1 (*Arg1*). Data are mean ± S.E. ($n = 3$/group). *, $p < 0.05$.

in M2 polarization, bone marrow macrophages were cocultured with CFSE-stained BAP or HAP RM-1 cells. After 5 h, flow cytometric analyses were performed to determine total efferocytosis, the population of F4/80+ macrophages that engulfed CFSE-stained RM-1 cells (*CFSE+F4/80+*), and M2 polarization (*F4/80+CD206+*) (Fig. 4*A*). Efferocytosis was significantly greater for HAP cells and occurred in conjunction with an increase in M2 macrophages. Similar results were also observed when bone marrow macrophages were cocultured with PC-3 cells (Fig. 4*B*). Although addition of rmMFG-E8 did not affect efferocytosis of tumor cells (data not shown), neutralizing antibody against MFG-E8 significantly inhibited efferocytosis of HAP cells and decreased M2 polarization of macrophages when compared with IgG controls (Fig. 4*C*). In summary, the flow cytometric analyses suggested that increased efferocytosis contributes to M2 polarization via MFG-E8. Moreover, neutralizing MFG-E8 antibody treatment significantly inhibited efferocytosis of HAP cells and reduced the HAP-induced M2 polarization, suggesting a unique role for MFG-E8.

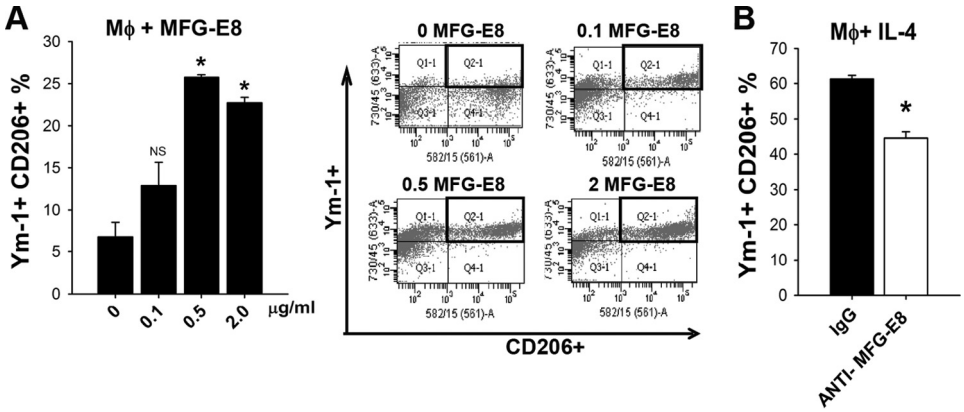

FIGURE 5. **MFG-E8 has a direct role in M2 macrophage polarization.** *A*, rmMFG-E8 treatment increased the M2 population in bone marrow macrophages. Bone marrow cells were expanded for three days with M-CSF and treated with rmMFG-E8 for 50 h at different concentrations (0–2 μg/ml). Shown are FACS analyses of M2 cells double-positive for CD206 and intracellular Ym-1. A representative FACS analysis is shown. Data are mean ± S.E. ($n = 4$/group). Two independent experiments were performed with similar results. *, $p < 0.05$. *NS*, not significant; *Mϕ*, bone marrow macrophages. *B*, IL-4-induced bone marrow macrophage M2 polarization (*Ym-1+ CD206+*) was reduced when cells were treated with anti-MFG-E8 antibody. Bone marrow macrophages were treated with 10 units/ml of IL-4 for 24 h in the presence of anti-MFG-E8 antibody (20 μg/ml) or IgG control. Data are mean ± S.E. ($n = 4$/group). *, $p < 0.05$.

To better determine the effect of cancer efferocytosis in macrophage activation and its participation in cancer inflammation, inflammatory protein array analyses were performed. Bone marrow macrophages were cultured in the presence or absence of HAP RM-1 for 24 h, and the supernatant proteins were analyzed (Fig. 4*D*). Interestingly, M2-related proteins (32, 33), such as IL-6, chemokine (C-C motif) ligand 2 (CCL2, also known as MCP-1), and chemokine (C-C motif) ligand 1 (CCL1, also known as TCA-3), were augmented significantly with efferocytosis. The production of CXC-chemokine family members such as KC, Lix, and XCL-1, as well as IL-13 and IL-17, were also significantly higher when macrophages were cultured with HAP RM-1 cells (data not shown). However, M1 related proteins such as GM-CSF, INF-γ, IL-1α and β, TNF-α, IL-12 p40/70, and IL-12P70 were not changed significantly (data not shown).

To further validate M2 polarization, M2 macrophage-associated genes were investigated when macrophages were cultured with HAP RM-1 tumor cells and at 4 °C to block efferocytosis (Fig. 4*E*). Expression of M2 macrophage-associated genes such as interleukin 10 (*Il10*), transforming growth factor β 1 (*Tgfb1*), Ym-1 (*Chi3l3*), and arginase 1 (*Arg1*) were decreased significantly when efferocytosis was blocked at 4 °C. Incubation at 4 °C did not alter gene expression, except arginase, which was increased significantly (Fig. 4*F*). Collectively, these data suggest that macrophage alternative activation into an M2 phenotype is facilitated by efferocytosis.

Direct Role of MFG-E8 in M2 Macrophage Polarization—Because rmMFG-E8 is also known to modulate macrophage responses (22), its direct role in macrophage polarization was investigated (Fig. 5). Bone marrow macrophages expanded for 3 days with M-CSF were treated with different concentrations of rmMFG-E8 protein for 50 h and analyzed by flow cytometry for the M2 markers mannose receptor CD206 and intracellular Ym-1 (Fig. 5*A*). Interestingly, bone marrow macrophages showed a dose-dependent increase in M2 polarization, reaching a peak at 0.5 μg/ml and decreasing at 2 μg/ml, an MFG-E8 concentration that has been reported to inhibit efferocytosis (16). To better clarify the direct role of MFG-E8, macrophages were treated with IL-4 to induce M2 polarization in the presence of anti-MFG-E8 antibody or IgG control (Fig. 5*B*). M2 polarization was reduced significantly with MFG-E8 neutralization. These data suggest that MFG-E8 may directly activate and modulate macrophage polarization into an M2 type.

STAT3 Pathway in MFG-E8-mediated Efferocytosis and M2 Polarization—MFG-E8 activates the JAK/STAT3 pathway in macrophages (22). Therefore, to determine whether the STAT3 pathway is important for MFG-E8-mediated efferocytosis, macrophages were treated for 2 h with the STAT3 inhibitor Stattic prior to coculture with tumor cells (Fig. 6, *A* and *B*). Stattic targets the STAT3-SH2 domain and prevents its association with upstream kinases, inhibiting cellular phosphorylation of STAT3 at Tyr-705 (34). Flow cytometric analyses revealed that phospho-STAT3 (p-STAT3) inhibition with Stattic pretreatment not only inhibited efferocytosis of RM-1 (Fig. 6*A*) and PC-3 (Fig. 6*B*) but also decreased M2 F4/80+CD206+ cells. To better delineate the role of MFG-E8 in efferocytosis and STAT3, macrophages from mutant MFG-E8 (KO) and control (WT) were given apoptosis-mimicking, PS-coated carboxylated beads, and the STAT3 pathway was investigated (Fig. 6, *C–E*). Phagocytosis of PS-coated beads was reduced significantly in MFG-E8 mutant (KO) mice, as expected (Fig. 6, *C* and *D*). The STAT3 pathway was investigated further in macrophages challenged with STAT3 inhibition or vehicle prior to phagocytosis with PS-coated carboxylated beads (Fig. 6*E*). Interestingly, macrophage phagocytosis stimulated phosphorylation of STAT3 and SOCS3 activation in WT compared with control non-stimulated macrophages. Inhibition of STAT3 phosphorylation by pretreatment with Stattic resulted in decreased STAT3 phosphorylation and a further increase in SOCS3 expression. MFG-E8 KO macrophage p-STAT3 levels were not changed after phagocytosis of PS-coated beads, and, even though inhibition of STAT3 was significant, no effect was observed in SOCS3 activation, suggesting that decreased phagocytosis in MFG-E8 KO blunted P-STAT3 activation and the SOCS3 response. Collectively, the data in Fig. 6 suggest that the STAT3 pathway is important for macrophage efferocytosis and

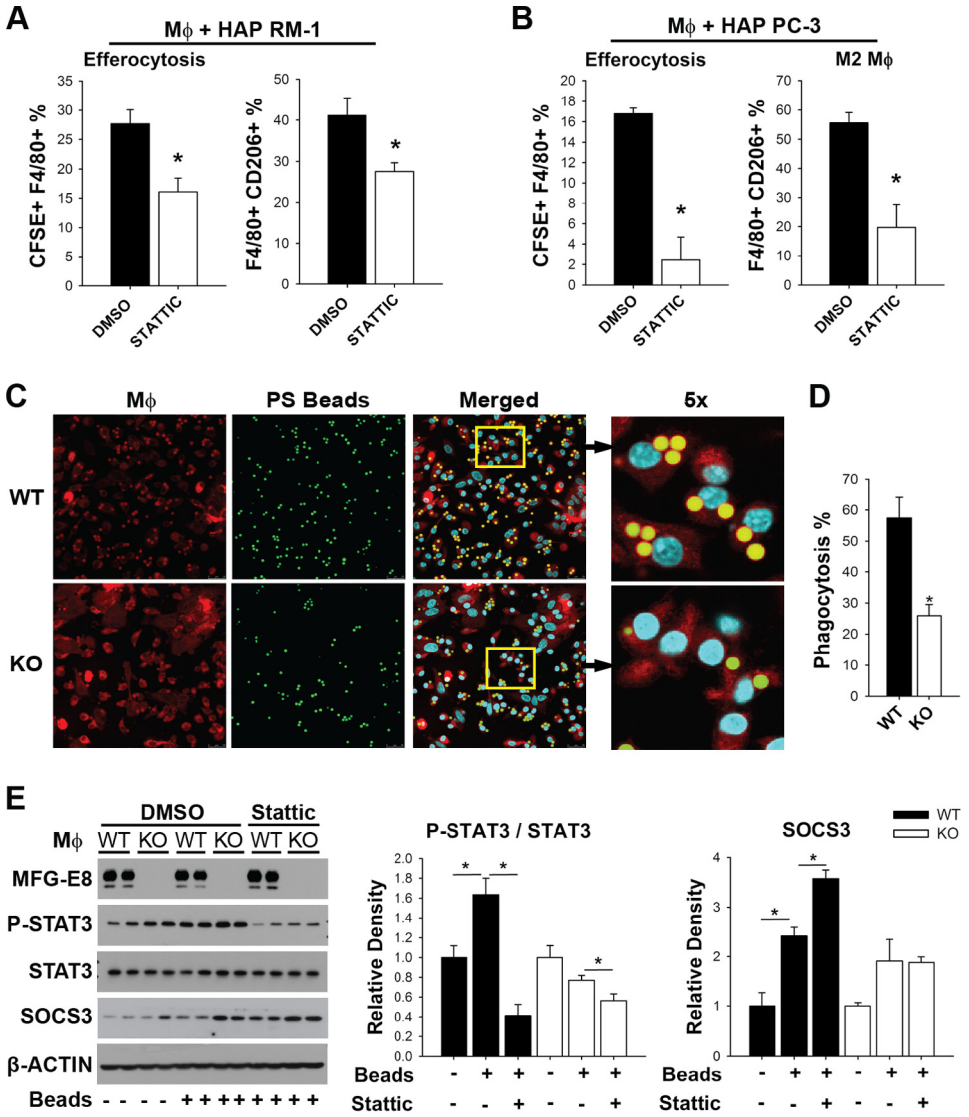

FIGURE 6. **Macrophage efferocytosis and activation of phospho-STAT3 signaling.** *A* and *B*, flow cytometric analyses for efferocytosis (*dual CFSE+F4/80+*) and M2 polarization (*F4/80+CD206+*). Macrophages (*Mϕ*) were pretreated with the phospho-STAT3 inhibitor Stattic 2 h prior to culture with RM-1 (*A*) and PC-3 (*B*) HAP tumor cells at a 1:3 ratio (*Mϕ:HAP*). Data are mean ± S.E. ($n = 4$/group). *, $p < 0.05$. Experiments were performed three times with similar results. *DMSO*, dimethyl sulfoxide. *C*, macrophages were cocultured with PS-coated carboxylated beads (1:2 ratio) for 1 h. Shown are representative confocal images of bone marrow macrophages (*red*) from WT or MFG-E8 mutant mice (KO) engulfing fluorescent carboxylated beads. DAPI (*blue*) was the nuclear stain. *D*, quantification of phagocytic index was calculated using the following formula: (number of engulfed beads / number of total Mϕ) × (Mϕ that engulfed beads/number of total Mϕ) × 100. Data are mean ± S.E. from two independent experiments, a total of $n = 7$/group. *, $p < 0.05$. *E*, representative Western blot showing two independent samples per group and the density quantification. Phospho-STAT3 expression levels were normalized to total STAT3 (*p-STAT3/STAT3*, $n = 4$/group), and SOCS3 ($n = 2$) expression levels were normalized relative to β-actin levels. Fold change was calculated for WT or MFG-E8 mutant mice (KO) dimethyl sulfoxide controls. Experiments were repeated twice, and data are mean ± S.E. *, $p < 0.05$.

M2 polarization. Furthermore, efferocytosis elicits phosphorylation of STAT3.

MFG-E8 and Efferocytosis in the STAT3/SOCS3 Pathway—The STAT3/SOCS3 pathway is important for cytokine expression in macrophages, playing essential roles in tumorigenesis and inflammation (35). SOCS3 is a negative regulator of STAT3 (36). Interestingly, Fig. 6*E* shows that STAT3 inhibition resulted in increased SOCS3 expression. Therefore, the relationship between p-STAT3 and SOCS3 was investigated further in the context of efferocytosis of tumor cells (Fig. 7). Macrophages were pretreated with Cytochalasin D, a potent inhibitor of actin polymerization and phagocytosis, or with dimethyl sulfoxide as a control for 2 h prior to incubation with HAP PC-3 cells. Efferocytosis inhibition with Cytochalasin D significantly suppressed p-STAT3 activation in macrophages stimulated with PC-3 HAP cells (Fig. 7*A*). SOCS3 demonstrated an opposite response to Cytochalasin D inhibition, with significantly increased SOCS3 expression in both WT and KO macrophages.

To further clarify the STAT3/SOCS3 pathway and the role of MFG-E8 in this process, WT and KO bone marrow macrophages were cultured with HAP RM-1 tumor cells expressing reduced MFG-E8 levels (GIPZ-control, *versus* knockdown shRNA m_08 or m_30 clones) (Fig. 7*B*). The purpose of modulating tumor-derived MFG-E8 was to determine whether paracrine MFG-E8 also played a role in the activation of macrophages and in the STAT3/SOCS3 pathway. Strikingly, macrophages cultured with shRNA knockdown clones pre-

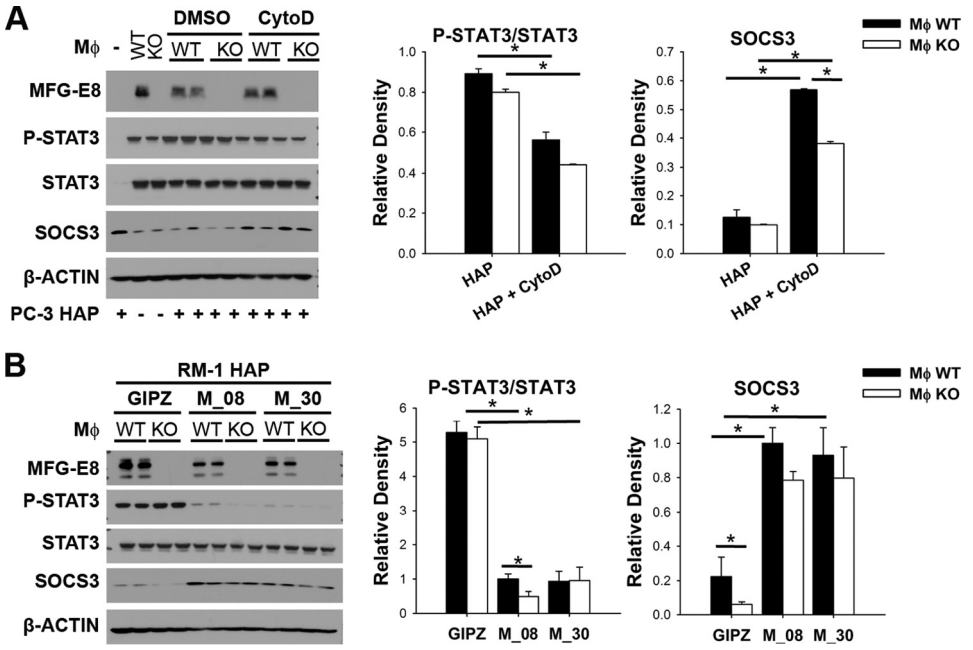

FIGURE 7. **MFG-E8 and efferocytosis in the STAT3/SOCS3 signaling pathway.** *A*, WT or MFG-E8 mutant (KO) macrophages were pretreated 2 h with the efferocytosis inhibitor Cytochalasin D (2 μM) or control dimethyl sulfoxide. Cells were then incubated with HAP PC-3 cells at a 1:3 ratio for 6 h. Western blot analysis was performed in two independent samples per group, and the relative expression to β-actin control was quantified. Phospho-STAT3 expression levels were normalized to total STAT3 (*p-STAT3/STAT3*). Data are mean ± S.E. (n = 2/group). *, $p < 0.05$. B, high apoptotic GIPZ (negative control) or MFG-E8 knockdown shRNA (*m_08* and *m_30*) RM-1 cells were incubated for 5 h at a 1:1 ratio. A representative image for Western blot analyses is shown, and p-STAT3 and SOCS3 expression was determined. Data are mean ± S.E. of two independent samples per group repeated twice (total n = 4/group). *, $p < 0.05$.

sented significantly reduced P-STAT3 activation and exacerbated SOCS3 activation compared with cells cultured with control GIPZ RM-1 cells, which had an opposite response. These data suggest that tumor-derived MFG-E8 is important for macrophage activation of the STAT3 pathway and that the SOCS3 pathway negatively regulates STAT3 activation, indicating that tumor cell efferocytosis impacts the STAT3/SOCS3 pathway in macrophages.

Collectively, the important roles of tumor cell efferocytosis in STAT3 activation suggest SOCS3 as a negative regulator of this pathway. Moreover, tumor-derived MFG-E8 may play important roles not only in efferocytosis but may also have a significant paracrine effect in the regulation of the STAT3/SOCS3 pathway.

DISCUSSION

Efferocytosis is an important process for maintaining homeostasis but may also have deleterious effects. Its role in the context of cancer and, specifically, skeletal metastases is intriguing yet unexplored. In normal bone, macrophages, known as "osteomacs," constitute one-sixth of the total cells and express specific markers: F4/80 and CD68 (37, 38). Interestingly, depletion of macrophages influences osteoblastic bone formation, bone healing, and hematopoietic niche maintenance (38–42). Although there is a growing body of literature on TAMs, little attention has been given to the phagocytic function of TAMs in the tumor environment and the mechanisms that control this process. In this study, the interactions of macrophages and tumor cells were investigated with a focus on efferocytosis and its effects on macrophage polarization via MFG-E8.

Clearance of apoptotic cells is essential to preserve tissue integrity and prevent the accumulation of harmful products released from dying cells. Deficient efferocytosis is associated with autoimmune diseases because of exacerbated and abnormal inflammatory responses (16, 17). Efferocytosis via MFG-E8 influences phagocytic cells such as macrophages and dendritic cells to down-regulate proinflammatory responses (22, 43). Furthermore, MFG-E8 has anti-inflammatory roles in homeostasis, evidenced by its modulation of proinflammatory signaling during efferocytosis through activation of the $\alpha_v\beta_3$ integrin receptors expressed by macrophages (18, 43, 44). Pretreatment of macrophages with the MFG-E8 recombinant protein resulted in reduced proinflammatory responses induced by LPS stimulation (22). Interestingly, in cancer, the protumorigenic macrophage also known as M2 alternatively activated (or TAM) shares many similarities with the phagocytic macrophage. TAMs have an anti-inflammatory role in the tumor microenvironment, expressing phagocytic markers such as mannose receptors (CD206) and anti-inflammatory cytokines and factors that not only participate in immunosuppression but also promote tumor growth (6). In this study, MFG-E8 was expressed in three different prostate cancer cell lines, and coculture of macrophages with cells undergoing apoptosis increased efferocytosis as well as MFG-E8 production.

MFG-E8 levels were found to have a direct effect on macrophage polarization. A key question in the activation of M2 TAMs is which signals drive protumorigenic polarization. MFG-E8 also has anti-inflammatory roles, capable of modulating inflammatory signaling during efferocytosis (18). Interest-

ingly, phagocytes activated by the interaction with apoptotic cells via MFG-E8 share similar anti-inflammatory and tumor-promoting properties, as seen in M2 TAMs (12). Coculture of macrophages with apoptotic cells induced macrophage polarization, as demonstrated by both flow cytometric analyses and quantitative PCR of M2-related genes. Interestingly, when efferocytosis was decreased via incubation at 4 °C or neutralizing MFG-E8 antibody treatment, M2 polarization was also reduced, suggesting that efferocytosis is important for macrophage polarization into tumor-promoting M2 cells. When macrophages were challenged with efferocytosis, increased secretion of M2-related cytokines such as IL-6 and CCL-2 (MCP-1) was observed (3, 45–47). Indeed, the observation that IL-6 is increased dramatically (> 20-fold) with efferocytosis further supports and explains our findings of STAT3 activation in this pathway. M1-related proteins were not changed significantly with efferocytosis. Furthermore, MFG-E8 may also directly mediate macrophage responses. Addition of rmMFG-E8 protein augmented macrophage polarization into an M2 macrophage, and this polarization was decreased significantly in the presence of the neutralizing antibody against MFG-E8.

The involvement of the STAT3/SOCS3 activation pathway in macrophage polarization was also investigated. The increase in MFG-E8 levels when bone marrow macrophages were cocultured with apoptotic cells was accompanied by SOCS3 down-regulation. SOCS3 deficiency in myeloid lineage cells has been shown to prolong activation of the JAK/STAT pathway and M1 polarization, suggesting that SOCS3 is required for M1 activation (22, 36, 48). SOCS3 down-regulation in macrophages by siRNA induced M2 polarization and activation of STAT3 (49). In addition, myeloid cell-specific SOCS3 conditional KO mice had fewer liver and lung metastatic nodules than the wild type in a mouse melanoma metastatic model (35). SOCS3 conditional KO myeloid cells stimulated with tumor lysates exhibited prolonged STAT3 phosphorylation with increased CCL8 (MCP2) production associated with the antitumor metastatic effect.

Here we demonstrated that inhibition of STAT3 signaling resulted in decreased efferocytosis and M2 polarization. In contrast, SOCS3 presented an opposite effect, with reduced expression when STAT3 was activated by efferocytosis and increased expression with efferocytosis and STAT3 inhibition. Taken together, we hypothesize that STAT3 participates in both efferocytosis and M2 polarization and that SOCS3 functions as a negative regulator of this pathway (Fig. 8).

A notable finding in this study was the fact that tumor-derived MFG-E8 may also play an important role in macrophages. The striking result of STAT3 reduction and SOCS3 activation in macrophages cultured with MFG-E8 knockdown cells indicates the importance of a paracrine effect that MFG-E8 may exert in macrophage activation and signaling. Still, the data suggest that MFG-E8 could not only be mediating efferocytosis and cell-cell interactions but could also be eliciting macrophage responses in an autocrine and paracrine manner.

Finally, MFG-E8 is not only expressed in multiple tissues but is also highly expressed in cancers such as malignant melanoma

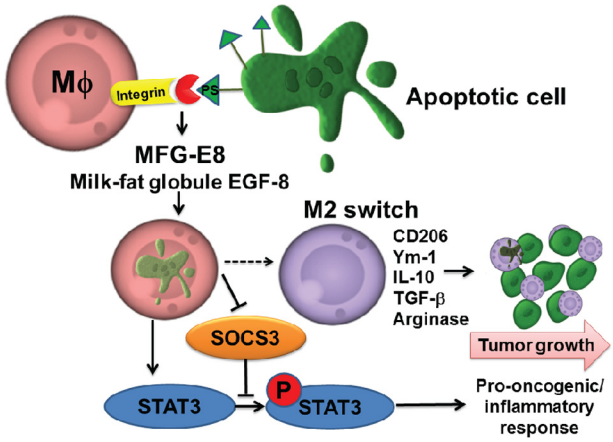

FIGURE 8. **Proposed model of MFG-E8-mediated efferocytosis of tumor cells and macrophage polarization.** MFG-E8 is a protein that functions as a bridge binding to the $\alpha_v\beta_3/\alpha_v\beta_5$ integrin expressed by macrophages and to PS externalized on apoptotic cells. Macrophages (*Mϕ*) interact with apoptotic cells, resulting in increased MFG-E8 expression, therefore mediating the efferocytosis of apoptotic tumor cells. This interaction activates the phosphorylation of STAT3, leading to a polarization of macrophages into M2 tumor-promoting macrophages with increased expression of M2 markers such as CD206 and Ym-1 as well as M2-related genes of cytokines and growth factors known to contribute to tumor promotion. Moreover, MFG-E8 and efferocytosis may inhibit SOCS3, a negative regulator of STAT3, therefore keeping STAT3 signaling activated and promoting M2 polarization.

and has been associated with tumor progression and growth (25, 50). Jinushi *et al.* (50) reported that MFG-E8 signals through Akt and Twist-dependent pathways to promote tumor growth and metastasis in malignant melanoma . They proposed MFG-E8 blockage as a potential therapeutic strategy. MFG-E8 antibody administration resulted in improved antitumor activities, such as radiation and chemotherapies, and elicited immune activation against tumor cells (25). Until now, MFG-E8 expression and involvement in prostate cancer had not been explored. In this study, it was demonstrated that patients with primary and metastatic prostate cancer had higher MFG-E8 expression in prostate tissue and blood exosomes compared with control patients. CD68+ macrophages in close proximity to MFG-E8-enriched areas of tumors were also augmented in malignant prostate cancer tissue. BPH tissues, which present a high turnover rate of prostate epithelia, are associated with increased macrophages and other inflammatory cells (51, 52). Macrophages contribute to the high proliferation rates and aggravate the chronic inflammatory state (53, 54). Although little is known about the efferocytic macrophages present in the BPH tissue regarding cell clearance, it is possible that they could be active players in this process. Interestingly, in this study, MFG-E8 expression was increased dramatically in the malignant tissues compared with BPH tissues. When macrophages were quantified, it was clear that malignant tissue presented an increased number of these cells in close proximity to the MFG-E8+ epithelial cells, which suggests potential efferocytic interactions compared with what was observed in the BPH cells. Therefore, a role for MFG-E8 in prostate cancer progression and growth is likely, and the findings from this study suggest that it is a potential candidate for therapeutic targeting. In conclusion, we report a novel mechanism by which MFG-E8, by mediating efferocytosis of prostate cancer cells, can support tumor growth

through facilitation of M2 macrophage polarization and regulation of SOCS3/STAT3 activation.

Acknowledgments—We thank Dr. Serk In Park (Vanderbilt University School of Medicine, Nashville, TN), Dr. Sun Wook Cho (National Medical Center, Seoul, Korea), and Drs. Mark and Kathy Day for advice, direction, and technical assistance. We also thank the University of Michigan Flow Cytometry Core for assistance with FACS analysis and the University of Michigan Microscopy and Imaging Analysis Facility for assistance with confocal microscopy imaging.

REFERENCES

1. Bubendorf, L., Schöpfer, A., Wagner, U., Sauter, G., Moch, H., Willi, N., Gasser, T. C., and Mihatsch, M. J. (2000) Metastatic patterns of prostate cancer: an autopsy study of 1,589 patients. *Hum. Pathol.* **31,** 578–583
2. Weilbaecher, K. N., Guise, T. A., and McCauley, L. K. (2011) Cancer to bone: a fatal attraction. *Nat. Rev. Cancer* **11,** 411–425
3. Li, X., Loberg, R., Liao, J., Ying, C., Snyder, L. A., Pienta, K. J., and McCauley, L. K. (2009) A destructive cascade mediated by CCL2 facilitates prostate cancer growth in bone. *Cancer Res.* **69,** 1685–1692
4. Loberg, R. D., Ying, C., Craig, M., Yan, L., Snyder, L. A., and Pienta, K. J. (2007) CCL2 as an important mediator of prostate cancer growth *in vivo* through the regulation of macrophage infiltration. *Neoplasia* **9,** 556–562
5. Loberg, R. D., Gayed, B. A., Olson, K. B., and Pienta, K. J. (2005) A paradigm for the treatment of prostate cancer bone metastases based on an understanding of tumor cell-microenvironment interactions. *J. Cell. Biochem.* **96,** 439–446
6. Park, S. I., Soki, F. N., and McCauley, L. K. (2011) Roles of bone marrow cells in skeletal metastases: no longer bystanders. *Cancer Microenviron.* **4,** 237–246
7. Pollard, J. W. (2009) Trophic macrophages in development and disease. *Nat. Rev. Immunol.* **9,** 259–270
8. Siveen, K. S., and Kuttan, G. (2009) Role of macrophages in tumour progression. *Immunol. Lett.* **123,** 97–102
9. Pollard, J. W. (2004) Tumour-educated macrophages promote tumour progression and metastasis. *Nat. Rev. Cancer* **4,** 71–78
10. Colotta, F., Allavena, P., Sica, A., Garlanda, C., and Mantovani, A. (2009) Cancer-related inflammation, the seventh hallmark of cancer: links to genetic instability. *Carcinogenesis* **30,** 1073–1081
11. Murdoch, C., Muthana, M., Coffelt, S. B., and Lewis, C. E. (2008) The role of myeloid cells in the promotion of tumour angiogenesis. *Nat. Rev. Cancer* **8,** 618–631
12. Gregory, C. D., and Pound, J. D. (2011) Cell death in the neighbourhood: direct microenvironmental effects of apoptosis in normal and neoplastic tissues. *J. Pathol.* **223,** 177–194
13. Reiter, I., Krammer, B., and Schwamberger, G. (1999) Cutting edge: differential effect of apoptotic versus necrotic tumor cells on macrophage antitumor activities. *J. Immunol.* **163,** 1730–1732
14. Savill, J., Dransfield, I., Gregory, C., and Haslett, C. (2002) A blast from the past: clearance of apoptotic cells regulates immune responses. *Nat. Rev. Immunol.* **2,** 965–975
15. Michlewska, S., Dransfield, I., Megson, I. L., and Rossi, A. G. (2009) Macrophage phagocytosis of apoptotic neutrophils is critically regulated by the opposing actions of pro-inflammatory and anti-inflammatory agents: key role for TNF-α. *FASEB J.* **23,** 844–854
16. Hanayama, R., Tanaka, M., Miwa, K., Shinohara, A., Iwamatsu, A., and Nagata, S. (2002) Identification of a factor that links apoptotic cells to phagocytes. *Nature* **417,** 182–187
17. Hanayama, R., Tanaka, M., Miyasaka, K., Aozasa, K., Koike, M., Uchiyama, Y., and Nagata, S. (2004) Autoimmune disease and impaired uptake of apoptotic cells in MFG-E8-deficient mice. *Science* **304,** 1147–1150
18. Miksa, M., Amin, D., Wu, R., Jacob, A., Zhou, M., Dong, W., Yang, W. L., Ravikumar, T. S., and Wang, P. (2008) Maturation-induced down-regulation of MFG-E8 impairs apoptotic cell clearance and enhances endotoxin response. *Int. J. Mol. Med.* **22,** 743–748
19. Asano, K., Miwa, M., Miwa, K., Hanayama, R., Nagase, H., Nagata, S., and Tanaka, M. (2004) Masking of phosphatidylserine inhibits apoptotic cell engulfment and induces autoantibody production in mice. *J. Exp. Med.* **200,** 459–467
20. Thorp, E., and Tabas, I. (2009) Mechanisms and consequences of efferocytosis in advanced atherosclerosis. *J. Leukocyte Biol.* **86,** 1089–1095
21. Lewis, C. E., and Pollard, J. W. (2006) Distinct role of macrophages in different tumor microenvironments. *Cancer Res.* **66,** 605–612
22. Aziz, M., Jacob, A., Matsuda, A., Wu, R., Zhou, M., Dong, W., Yang, W. L., and Wang, P. (2011) Pre-treatment of recombinant mouse MFG-E8 downregulates LPS-induced TNF-α production in macrophages via STAT3-mediated SOCS3 activation. *PLoS ONE* **6,** e27685
23. Yoshimura, A., Naka, T., and Kubo, M. (2007) SOCS proteins, cytokine signalling and immune regulation. *Nat. Rev. Immunol.* **7,** 454–465
24. Atabai, K., Fernandez, R., Huang, X., Ueki, I., Kline, A., Li, Y., Sadatmansoori, S., Smith-Steinhart, C., Zhu, W., Pytela, R., Werb, Z., and Sheppard, D. (2005) Mfge8 is critical for mammary gland remodeling during involution. *Mol. Biol. Cell* **16,** 5528–5537
25. Jinushi, M., Sato, M., Kanamoto, A., Itoh, A., Nagai, S., Koyasu, S., Dranoff, G., and Tahara, H. (2009) Milk fat globule epidermal growth factor-8 blockade triggers tumor destruction through coordinated cell-autonomous and immune-mediated mechanisms. *J. Exp. Med.* **206,** 1317–1326
26. Lin, D. L., Tarnowski, C. P., Zhang, J., Dai, J., Rohn, E., Patel, A. H., Morris, M. D., and Keller, E. T. (2001) Bone metastatic LNCaP-derivative C4–2B prostate cancer cell line mineralizes *in vitro*. *Prostate* **47,** 212–221
27. Cho, S. W., Pirih, F. Q., Koh, A. J., Michalski, M., Eber, M. R., Ritchie, K., Sinder, B., Oh, S., Al-Dujaili, S. A., Lee, J., Kozloff, K., Danciu, T., Wronski, T. J., and McCauley, L. K. (2013) The soluble interleukin-6 receptor is a mediator of hematopoietic and skeletal actions of parathyroid hormone. *J. Biol. Chem.* **288,** 6814–6825
28. Koh, A. J., Novince, C. M., Li, X., Wang, T., Taichman, R. S., and McCauley, L. K. (2011) An irradiation-altered bone marrow microenvironment impacts anabolic actions of PTH. *Endocrinology* **152,** 4525–4536
29. Novince, C. M., Michalski, M. N., Koh, A. J., Sinder, B. P., Entezami, P., Eber, M. R., Pettway, G. J., Rosol, T. J., Wronski, T. J., Kozloff, K. M., and McCauley, L. K. (2012) Proteoglycan 4: a dynamic regulator of skeletogenesis and parathyroid hormone skeletal anabolism. *J. Bone Miner. Res.* **27,** 11–25
30. Vlassov, A. V., Magdaleno, S., Setterquist, R., and Conrad, R. (2012) Exosomes: current knowledge of their composition, biological functions, and diagnostic and therapeutic potentials. *Biochim. Biophys. Acta* **1820,** 940–948
31. Aziz, M., Jacob, A., Matsuda, A., and Wang, P. (2011) Review: milk fat globule-EGF factor 8 expression, function and plausible signal transduction in resolving inflammation. *Apoptosis* **16,** 1077–1086
32. Mantovani, A., Sica, A., Sozzani, S., Allavena, P., Vecchi, A., and Locati, M. (2004) The chemokine system in diverse forms of macrophage activation and polarization. *Trends Immunol.* **25,** 677–686
33. Locati, M., Mantovani, A., and Sica, A. (2013) Macrophage activation and polarization as an adaptive component of innate immunity. *Adv. Immunol.* **120,** 163–184
34. Schust, J., Sperl, B., Hollis, A., Mayer, T. U., and Berg, T. (2006) Stattic: a small-molecule inhibitor of STAT3 activation and dimerization. *Chem. Biol.* **13,** 1235–1242
35. Hiwatashi, K., Tamiya, T., Hasegawa, E., Fukaya, T., Hashimoto, M., Kakoi, K., Kashiwagi, I., Kimura, A., Inoue, N., Morita, R., Yasukawa, H., and Yoshimura, A. (2011) Suppression of SOCS3 in macrophages prevents cancer metastasis by modifying macrophage phase and MCP2/CCL8 induction. *Cancer Lett.* **308,** 172–180
36. Dimitriou, I. D., Clemenza, L., Scotter, A. J., Chen, G., Guerra, F. M., and Rottapel, R. (2008) Putting out the fire: coordinated suppression of the innate and adaptive immune systems by SOCS1 and SOCS3 proteins. *Immunol. Rev.* **224,** 265–283
37. Austyn, J. M., and Gordon, S. (1981) F4/80, a monoclonal antibody directed specifically against the mouse macrophage. *Eur. J. Immunol.* **11,** 805–815
38. Pettit, A. R., Chang, M. K., Hume, D. A., and Raggatt, L. J. (2008) Osteal macrophages: a new twist on coupling during bone dynamics. *Bone* **43,**

976–982
39. Chang, M. K., Raggatt, L. J., Alexander, K. A., Kuliwaba, J. S., Fazzalari, N. L., Schroder, K., Maylin, E. R., Ripoll, V. M., Hume, D. A., and Pettit, A. R. (2008) Osteal tissue macrophages are intercalated throughout human and mouse bone lining tissues and regulate osteoblast function *in vitro* and *in vivo*. *J. Immunol.* **181,** 1232–1244
40. Winkler, I. G., Sims, N. A., Pettit, A. R., Barbier, V., Nowlan, B., Helwani, F., Poulton, I. J., van Rooijen, N., Alexander, K. A., Raggatt, L. J., and Lévesque, J. P. (2010) Bone marrow macrophages maintain hematopoietic stem cell (HSC) niches and their depletion mobilizes HSCs. *Blood* **116,** 4815–4828
41. Alexander, K. A., Chang, M. K., Maylin, E. R., Kohler, T., Müller, R., Wu, A. C., Van Rooijen, N., Sweet, M. J., Hume, D. A., Raggatt, L. J., and Pettit, A. R. (2011) Osteal macrophages promote in vivo intramembranous bone healing in a mouse tibial injury model. *J. Bone Miner. Res.* **26,** 1517–1532
42. Cho, S. W., Soki, F. N., Koh, A. J., Eber, M. R., Entezami, P., Park, S. I., van Rooijen, N., and McCauley, L. K. (2014) Osteal macrophages support physiologic skeletal remodeling and anabolic actions of parathyroid hormone in bone. *Proc. Natl. Acad. Sci. U.S.A.* **111,** 1545–1550
43. Aziz, M. M., Ishihara, S., Mishima, Y., Oshima, N., Moriyama, I., Yuki, T., Kadowaki, Y., Rumi, M. A., Amano, Y., and Kinoshita, Y. (2009) MFG-E8 attenuates intestinal inflammation in murine experimental colitis by modulating osteopontin-dependent $\alpha v\beta 3$ integrin signaling. *J. Immunol.* **182,** 7222–7232
44. Brissette, M. J., Lepage, S., Lamonde, A. S., Sirois, I., Groleau, J., Laurin, L. P., and Cailhier, J. F. (2012) MFG-E8 released by apoptotic endothelial cells triggers anti-inflammatory macrophage reprogramming. *PLoS ONE* **7,** e36368
45. Roca, H., Varsos, Z. S., Sud, S., Craig, M. J., Ying, C., and Pienta, K. J. (2009) CCL2 and interleukin-6 promote survival of human CD11b+ peripheral blood mononuclear cells and induce M2-type macrophage polarization. *J. Biol. Chem.* **284,** 34342–34354
46. Fernando, M. R., Reyes, J. L., Iannuzzi, J., Leung, G., and McKay, D. M. (2014) The pro-inflammatory cytokine, interleukin-6, enhances the polarization of alternatively activated macrophages. *PLoS ONE* **9,** e94188
47. Zhang, J., Patel, L., and Pienta, K. J. (2010) CC chemokine ligand 2 (CCL2) promotes prostate cancer tumorigenesis and metastasis. *Cytokine Growth Factor Rev.* **21,** 41–48
48. Qin, H., Holdbrooks, A. T., Liu, Y., Reynolds, S. L., Yanagisawa, L. L., and Benveniste, E. N. (2012) SOCS3 deficiency promotes M1 macrophage polarization and inflammation. *J. Immunol.* **189,** 3439–3448
49. Liu, Y., Stewart, K. N., Bishop, E., Marek, C. J., Kluth, D. C., Rees, A. J., and Wilson, H. M. (2008) Unique expression of suppressor of cytokine signaling 3 is essential for classical macrophage activation in rodents *in vitro* and *in vivo*. *J. Immunol.* **180,** 6270–6278
50. Jinushi, M., Nakazaki, Y., Carrasco, D. R., Draganov, D., Souders, N., Johnson, M., Mihm, M. C., and Dranoff, G. (2008) Milk fat globule EGF-8 promotes melanoma progression through coordinated Akt and Twist signaling in the tumor microenvironment. *Cancer Res.* **68,** 8889–8898
51. Wang, X., Lin, W. J., Izumi, K., Jiang, Q., Lai, K. P., Xu, D., Fang, L. Y., Lu, T., Li, L., Xia, S., and Chang, C. (2012) Increased infiltrated macrophages in benign prostatic hyperplasia (BPH): role of stromal androgen receptor in macrophage-induced prostate stromal cell proliferation. *J. Biol. Chem.* **287,** 18376–18385
52. Fujii, T., Shimada, K., Asai, O., Tanaka, N., Fujimoto, K., Hirao, K., and Konishi, N. (2013) Immunohistochemical analysis of inflammatory cells in benign and precancerous lesions and carcinoma of the prostate. *Pathobiology* **80,** 119–126
53. Josson, S., Matsuoka, Y., Chung, L. W., Zhau, H. E., and Wang, R. (2010) Tumor-stroma co-evolution in prostate cancer progression and metastasis. *Semin. Cell Dev. Biol.* **21,** 26–32
54. De Nunzio, C., Kramer, G., Marberger, M., Montironi, R., Nelson, W., Schröder, F., Sciarra, A., and Tubaro, A. (2011) The controversial relationship between benign prostatic hyperplasia and prostate cancer: the role of inflammation. *Eur. Urol.* **60,** 106–117